Bezafibrate prevents palmitate-induced apoptosis in osteoblastic MC3T3-E1 cells through the NF-κB signaling pathway

XING ZHONG[1,2*], LINGLING XIU[1*], GUOHONG WEI[1], TIANRONG PAN[2], YUANYUAN LIU[1], LEI SU[1], YANBING LI[1] and HAIPENG XIAO[1]

[1]Department of Endocrinology, The First Affiliated Hospital, Sun Yat-sen University, Guangzhou, Guangdong 510080; [2]Department of Endocrinology, The Second Affiliated Hospital of Anhui Medical University, Hefei, Anhui 230601, P.R. China

Abstract. Osteoporosis is a bone condition defined by low bone mass and increase of fracture risk due to imbalance between bone resorption by osteoclasts and bone formation by osteoblasts. Low bone mass is likely to be due to the alteration of the osteoclast and osteoblast lifespan through regulated apoptosis. Saturated fatty acid (SFA) intake is negatively associated with bone mineral density (BMD). Furthermore, SFA induces apoptosis in osteoblastic cell lines. Bezafibrate could increase bone mass in intact male rats principally through increasing periosteal bone formation. At present, it is unknown whether bezafibrate attenuates palmitate-induced apoptosis in MC3T3-E1 cells. In the present study, we found that palmitate stimulated the degradation of IκBα and NF-κB translocation, as well as up-regulation of NF-κB-mediated Fas expression in obsteoblastic MC3T3-E1 cells. Furthermore, the NF-κB inhibitor pyrrolidine dithiocarbamate (PDTC) could restore palmitate-induced caspase-3 decrease and inhibit palmitate-induced cleaved caspase-3 increase. We observed that bezafibrate, a dual ligand for the peroxisome proliferator-activated receptors α (PPARα) and PPARδ, significantly attenuated the palmitate-induced cytotoxicity as determined by the MTT assay and inhibited the palmitate-induced apoptosis as determined by a flow cytometry assay using Annexin V-FITC/PI and assessment of the activity of caspase-3. Pre-treatment of bezafibrate prevented palmitate-induced NF-κB activation. Therefore, these findings indicate that bezafibrate inibits palmitate-induced apoptosis via the NF-κB signaling pathway. Our results point to bezafibrate as a new strategy to attenuate bone loss associated with high fat diet beyond its lipid-lowering actions.

Correspondence to: Professor Haipeng Xiao, Department of Endocrinology, The First Affiliated Hospital, Sun Yat-sen University, Guangzhou, Guangdong 510080, P.R. China
E-mail: xiaohp@mail.sysu.edu.cn

*Contributed equally

Introduction

Osteoporosis is a major public health concern that is characterized by low bone mineral density (BMD) and compromised bone strength, which predisposes the patient to increased fracture risk with high morbidity and mortality (1). Bone mass is determined by bone cell differentiation, activity, and death, which mainly occur through apoptosis. Increasing evidence demonstrates a possible link between apoptosis and osteoporosis. In bone, estrogen deficiency has been associated with accelerated osteoblast apoptosis and susceptibility to osteoporotic fractures. Increased osteocyte apoptosis is also observed in estrogen deficiency (2). In addition, long-term glucocorticoid therapy may lead to bone loss through multiple mechanisms, such as impaired calcium intestinal absorption, suppressed osteoblastic formation, and increased osteocyte apoptosis (3). Thus, the decrease in osteoblast number and bone formation rate in glucocorticoid excess may be explained in part by increased osteoblast apoptosis (4). These previous studies suggest that dysregulated apoptosis contributes to reduced bone mineral density.

An observational study has shown that high intake of saturated fatty acids (SFA) is positively associated with increased levels of blood cholesterol (5). Free fatty acids (FFA) are a major secretory product of adipocytes as a result of lipolysis of stored triglycerides. Palmitate is the most abundant fatty acid *in vivo*, accounting for ~26% of the total plasma fatty acids (6). Palmitic acid and stearic acid are also universally found in natural fats. Analysis of data from the third National Health and Nutrition Examination Survey (NHANES III) have shown that SFA intake is negatively associated with BMD (7). The Women's Health Initiative (WHI) study has shown that SFA intake may significantly increase hip fracture risk (8). Additionally, Makovey *et al* (9) reported a modest inverse relationship between lumbar spine and whole body BMD and serum total cholesterol (TC) and low-density lipoprotein (LDL) levels in post-menopausal women. Several animal studies also found that high-fat diet (HFD) has been to be detrimental to either bone quantity or quality (10) and reduces the BMD in female C57BI/6J aging mice (11). Thus, SFA may alter the balance of bone remodeling resulting in osteoporosis.

Cell culture studies have demonstrated that palmitate induces apoptosis in a variety of cell types, including osteoblastic cell lines (12). Palmitate induced a 2-fold increase in NF-κB activation and NF-κB inhibitor Bay 11-7085 attenuated palmitate-induced caspase-3 activation in cultured bovine retinal pericytes (13). Various factors including TNFα and serum deprivation could induce cell apoptosis through NF-κB activation in MC3T3-E1 cells (14,15). Thus, it is quite possible that palmitate-induced apoptosis in MC3T3-E1 cells is mediated by NF-κB activation.

Fibrate use, including bezafibrate, has been associated with a reduced odds of vertebral fracture in men and women (16). Moreover, an animal study has shown that lipid lowering by bezafibrate alleviated steroid-induced osteoporosis to the same degrees as statin (17). Another study has found that bezafibrate could increase bone mass in intact male rats principally through increasing periosteal bone formation (18). These results suggest that bezafibrate plays an important role in bone metabolism.

In this study, we examined whether palmitate-induced apoptosis of osteoblastic MC3T3-E1 cells is NF-κB dependent and whether bezafibrate can attenuate the palmitate-induced apoptosis in MC3T3-E1 cells.

Materials and methods

Reagents and chemicals. Chemicals including bezafibrate, pyrrolidine dithiocarbamate (PDTC), and palmitate were purchased from Sigma-Aldrich (St. Louis, MO). Fetal bovine serum (FBS), L-glutamine, penicillin/streptomycin, and α-minimal essential medium (α-MEM) were obtained from Gibco-BRL (Grand Island, NY). For Western blot analysis, phospho-NF-κB p65, total NF-κB p65, IκBα, caspase-3, cleaved caspase-3, and tubulin antibodies were purchased from Cell Signaling Technology (Danvers, MA). All other chemicals were of the highest grade available commercially.

Cell culture. MC3T3-E1 cells, a mouse osteoblastic cell line, were kindly provided by Professor Eryuan Liao (19). MC3T3-E1 cells were cultured in α-MEM supplemented with 10% FBS and 1% penicillin-streptomycin in 5% CO_2 at 37°C. After the cells had reached 80% confluence, the culture medium was replaced with a fresh medium that was supplemented with various concentrations of bezafibrate and/or palmiltate, and incubated for various time points.

Preparation of palmitic acid/BSA complex solution. The palmitate-BSA solution was prepared as previously described (20). Briefly, the sodium salt of palmitate was dissolved at a concentration of 10 mM in 11% (w/v) BSA in a shaking water-bath at 37°C overnight. The BSA was free of fatty acids and endotoxins. The pH of the solution was adjusted to 7.2~7.4 with 1 mM NaOH. The solution was filtered through a 0.2 μm filter and stored at -20°C. The palmitate-BSA was diluted to 1:20 in α-MEM medium, the molar ratio of palmitate to BSA being 6:1. Control cells were carried out in α-MEM containing FFA-free BSA.

Measurement of cell viability. Cell viability was determined by the 3-(4,5-dimethylthiazol-2-yl)-2,5-diphenyl tetrazolium

bromide (MTT) (Sigma-Aldrich, St. Louis, MO). Briefly, at the end of treatment, 10 μl of MTT was added to each well of a 96-well microplate and placed in an incubator at 37°C for 4 h. Dimethyl sulfoxide (DMSO) of 150 μl was added to all the wells and mixed thoroughly to lyse the cells and dissolve the dark blue crystals. After 10 min, the absorbance was measured at 570 nm using a microplate reader (Bio-Rad iMARK; Japan).

Annexin-V FITC staining apoptosis assay. Annexin V-FITC and PI staining were performed according to the recommended protocol and the cells were analyzed by flow cytometry (Becton-Dickinson, San Jose, CA). Briefly, cells were harvested by trypsinization, and resuspended in 1X binding buffer (0.1 M HEPES/NaOH, 1.4 M NaCl, 25 mM $CaCl_2$) at a concentration of $1x10^6$ cells/ml. The cell solution (100 μl, $1x10^5$ cells) were transferred to a 5 ml culture tube, and incubated with 5 μl of Annexin V-FITC and 5 μl PI for 15 min at 25°C in the dark. After incubation, 400 μl of 1X binding buffer was added to each tube and cells were analyzed by flow cytometry within 1 h. Cells that stain positive for Annexin V-FITC and negative for PI are undergoing apoptosis. Cells that stain positive for both Annexin V-FITC and PI are undergoing necrosis. Cells that stain negative for both Annexin V-FITC and PI are alive.

RNA preparation and real-time PCR. To investigate the expression of Fas ligand (FasL), Fas and β-actin mRNA in MC3T3-E1 cells, SYBR-Green chemistry was used to perform quantitative determinations of the mRNAs. Total-RNA was extracted from cultured MC3T3-E1 cells using TRIzol reagent (Invitrogen, San Diego, CA) according to the manufacturer's recommended protocol. The concentration and purity of total-RNA were calculated with absorbance at 260 and 280 nm. Total-RNA (1 μg) was employed for the synthesis of first strand cDNA (cDNA synthesis kit; Toyobo, Japan). Real-time PCR was performed using 1 μl of cDNA in a 25 μl reaction volume with ABI PRISM 7500 (Applied Biosystems, USA). The double-stranded DNA-specific dye SYBR-Green I was incorporated into the PCR buffer provided in the SYBR-Green PCR kit (Toyobo, Japan) to allow for quantitative detection of the PCR product. The PCR reactions were carried out under the following conditions: 95°C for 60 sec, 40 cycles at 95°C for 15 sec, 60°C for 15 sec and 72°C for 45 sec. All reactions were run in triplicate and analyzed by the $2^{-\Delta\Delta CT}$ method. PCR primers were designed using the Primer 5.0 software. The specific primers are as follows: β-actin, forward, 5'-TCTTG GGTATGGAATCCTGTG-3' and reverse, 5'-AGGTCTTTA CGGATGTCAACG-3' (82 bp); FasL, forward, 5'-ATGGTTC TGGTGGCTCTGGTT-3' and reverse, 5'-ATACTTTAAGGC TTTGGTTGGTG-3' (109 bp); Fas, forward, 5'-ATGGTTCT GGTGGCTCTGGTT-3' and reverse, 5'-ATAGGCGATTTCT GGGACTTTGT-3' (124 bp).

Preparation of nuclear protein extracts. Nuclear extracts were prepared from the cultured MC3T3-E1 cells for 2 h after palmitate with or without bezafibrate treatment according to the method of Iwata *et al* (21). Briefly, the cultured cells collected in 1 ml of Tris-buffered saline (25 mM Tris-HCl (pH 7.4), 130 mM NaCl and 5 mM KCl) were centrifuged at 7,000 x g for 30 sec. The pellet was suspended in 400 μl of

buffer A (10 mM HEPES (pH 7.9), 10 mM KCl, 0.1 mM EDTA, 0.1 mM EGTA, 1 mM dithiothreitol and 1 mM phenyl-methylsulfonyl fluoride). The suspension was placed on ice for 15 min. Then 30 µl of 10% NP-40 was added, and vigorously mixed for 10 sec. The nuclear fraction was precipitated in 50 µl of ice-cold buffer B (20 mM HEPES (pH 7.9), 400 mM NaCl, 1 mM phenylmethylsulfonyl fluoride). The mixture was placed on ice for 15 min with frequent agitation. Then the supernatants of the nuclear extracts were prepared by centri-fugation at 15,000 x g for 5 min and stored in aliquots at -80˚C. The protein concentration was determined by the BCA protein assay (Bio-Rad, Mississauga, ON, Canada).

Preparation of total protein extracts and Western blot analysis. For Western blotting, MC3T3-E1 cells were plated in 6 cm dish. Cells were washed twice with ice-cold PBS, then resuspended in lysis buffer (RIPA, Beyone, China) containing 1% NP-40, 0.1% SDS, 5 mM EDTA, 0.5% sodium deoxycholate, 1 mM sodium orthovanadate and 1 mmol/l phenylmethyl sulfonyl-fluoride. The cell lysates were then sonicated for 30 sec. For each sample, 30 µg protein, assessed by BCA protein assay, were run on a 10% polyacrylamide gel and transferred to a polyvinylidene difluoride (PVDF) membrane (Millipore, USA). After blocking with 5% non-fat milk/TBST, the membrane was incubated overnight at 4˚C with phospho-NF-κB p65, IκBα, caspase-3, and cleaved caspase-3 antibodies at 1:1,000 dilution. Specific antibody binding was detected by a 1:2,000 dilution of the corresponding horseradish peroxidase-conjugated secondary antibodies (Cell Signaling Technology) for 1 h at room temperature. The blots were then washed, and the signal was visualized by an HRP chemiluminescent substrate reagent kit (Invitrogen) according to the manufacturer's protocol. After stripping of phospho-NF-κB p65, NF-κB p65 immuno-reactivity was determined in the same membrane. The band intensity was quantified by densitometric analysis using the ImageJ software (National Institutes of Health, USA).

Immunofluorescence microscopy. MC3T3-E1 cells were cultured on cell culture coverslips (Nalge Nunc, Rochester, NY, USA). The cells were fixed in 4% paraformaldehyde/PBS for 30 min and then washed in PBS. After permeabilization with 0.2% Triton X-100/PBS for 15 min, cells were washed with PBS and blocked with blocking buffer (PBS with 1% BSA) at room temperature for 1 h followed by incubation with NF-κB p65 antibody (Cell Signaling Technology) at 4˚C overnight. After washing with PBS, the cells were incubated with Cy3-conjugated Affinipure goat anti-rabbit IgG (Proteintech, Chicago, IL, USA) diluted 200-fold in blocking buffer for 1 h at room temperature. They were then washed with PBS and incubated with DAPI (10 µg/ml) for 10 min to detect nuclear counterstaining. The slides were immediately visualized using Olympus fluorescence microscope (Olympus, Japan).

Statistical analysis. Data are expressed as the mean ± SEM and analyzed by SPSS 16.0 software. Statistical evaluations for differences between groups were performed by two-tailed independent Student's t-tests or one-way analysis of variance (ANOVA) followed by the Fisher's protected least significant difference (PLSD). P-values <0.05 were considered statistically significant.
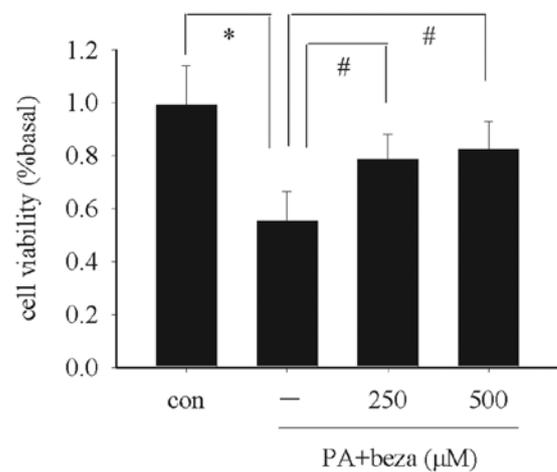

Figure 1. Effect of bezafibrate on palmitate-induced cytotoxicity in MC3T3-E1 cells. The cells were treated with 500 µM palmitate in the presence or absence of 250-500 µM bezafibrate for 24 h. Cell viability was determined using the MTT assay. Data are normalized to the average value of control and expressed as the mean ± SEM. (n=3). *P<0.05 vs. control; #P<0.05 vs. palmitate 500 µM alone.

Results

Effect of bezafibrate on palmitate-induced cytotoxicity in MC3T3-E1 cells. To investigate whether bezafibrate attenuates palmitate-induced cytotoxicity in MC3T3-E1 cells, cell viability was assessed using the MTT assay. Cells treated with 500 µM palmitate for 24 h reduced cell viability by 43% compared to control. When palmitate-exposed cells were treated with bezafibrate (250 and 500 µM), significant increases in cell viability were observed (Fig. 1). These results indicated that bezafibrate significantly attenuates palmitate-induced cyto-toxicity in MC3T3-E1 cells.

Effect of bezafibrate on palmitate-induced apoptosis in MC3T3-E1 cells. We investigated the effect of bezafibrate on palmitate-induced apoptosis by flow cytometry analysis. As shown in Fig. 2, untreated MC3T3-E1 cells were used as the control and palmitate significantly induced cell apoptosis. However, bezafibrate could significantly attenuate palmitate-induced apoptosis (34.08±6.61 vs. 16.03±3.47%, P<0.05). Furthermore, we examined palmitate-induced apoptosis by determining the expression of cleaved caspase-3 protein. Because caspase-3 has been implicated as a common downstream effector of diverse apoptotic pathways, we measured caspase-3 and cleaved caspase-3 protein expression (Fig. 3A). Caspase-3 expression was decreased by 34% with palmitate treatment and bezafibrate restored the palmitate-induced caspase-3 decrease (Fig. 3B). Cleaved caspase-3 levels increased by 1.98-fold with palmitate treatment and this increases was inhibited by bezafibrate (Fig. 3C). Taken together, the detection of phosphatidylserine externalization and caspase-3 activation suggest that bezafibrate could attenuate palmitate-induced apoptosis in MC3T3-E1 osteoblastic cells.

Effect of palmitate on Fas and FasL mRNA expression in MC3T3-E1 cells. To examine whether palmitate-induced apoptosis in MC3T3-E1 cells involves Fas and FasL, we
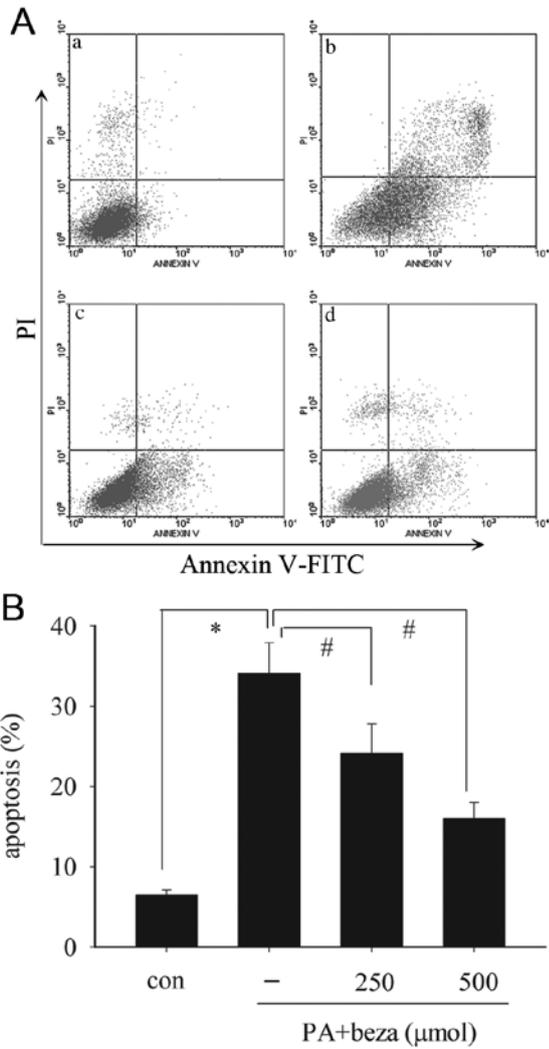
Figure 2. Effect of bezafibrate on palmitate-induced apoptosis in MC3T3-E1 cells. The cells were treated with 500 μM palmitate in the presence or absence of 250-500 μM bezafibrate for 24 h. (A) Flow cytometric analyses of MC3T3-E1 cells after Annexin V-FITC/PI double staining. The typical figures of flow cytometric analyses for apoptotic and necrotic cells. (a) control cells; (b) cells treated with 500 μM palmitate; cells treated with 500 μM palmitate and (c) 250 μM or (d) 500 μM bezafibrate. (B) Quantification of the flow cytometry analysis. Data are expressed as mean ± SEM. (n=3). *P<0.05 vs. control; #P<0.05 vs. palmitate alone.

Figure 3. Effect of bezafibrate on palmitate-induced cleaved caspase-3 in MC3T3-E1 cells. The cells were treated with 500 μM palmitate in the presence or absence of 250 or 500 μM bezafibrate for 24 h. (A) Levels of caspase-3 and cleaved caspase-3 protein expression were determined using Western blot analysis. (B) Quantification of caspase-3 and (C) cleaved caspase-3 protein expression levels are shown. Data are normalized to the average value of the control and expressed as mean ± SEM. (n=3). *P<0.05 vs. control; #P<0.05 vs. palmitate alone.

measured the expression of Fas and FasL mRNA by using real-time PCR. The expression of Fas mRNA was significantly higher in the palmitate treatment group compared to the control (Fig. 4A). Pre-treatment with 500 μM bezafibrate for 2 h before addition of palmitate decreased the expression of Fas mRNA by 33% compared to palmitate alone. However, exposure of MC3T3-E1 cells to palmitate did not modify the level of FasL mRNA expression.

Effect of palmitate on the NF-κB pathway in MC3T3-E1 cells. In resting cells, NF-κB is found in an inactive cytosolic form, retained by association with its inhibitor, IκB. Upon activation, IκB is rapidly phosphorylated, ubiquitinated, and degraded, releasing the active NF-κB complex to translocate into the nucleus. To determine whether palmitate activates the NF-κB signaling pathway in MC3T3-E1 cells, we measured the levels
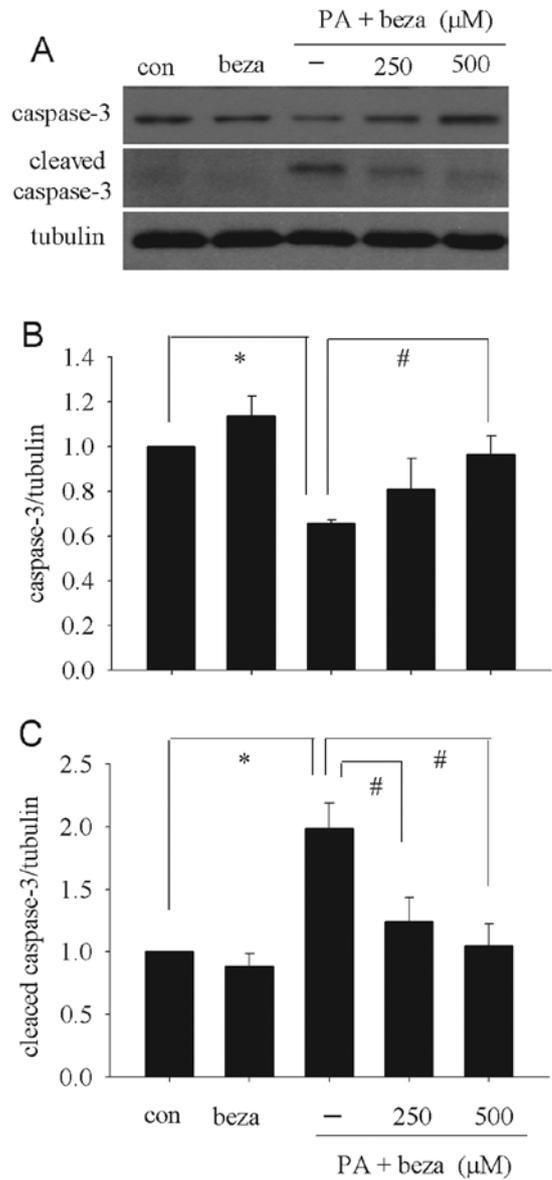
of IκBα, phospho-NF-κB p65 and total NF-κB p65 in total protein extracts from cells treated with palmitate for the indicated time. Levels of phospho-NF-κB p65 protein were markedly increased 60 min after stimulation with palmitate from very low levels and reached an ~2.96-fold increase of the baseline level at 120 min (Fig. 5A). IκBα levels were markedly reduced 60 min after stimulation with palmitate and decreased ~57% at 120 min (Fig. 5B).

To further address whether the NF-κB signaling pathway is involved in palmitate-induced osteoblast apoptosis, we pretreated MC3T3-E1 cells with the NF-κB inhibitor PDTC (Fig. 6). Compared to the group treated with palmitate alone, PDTC significantly restored palmitate-induced caspase-3
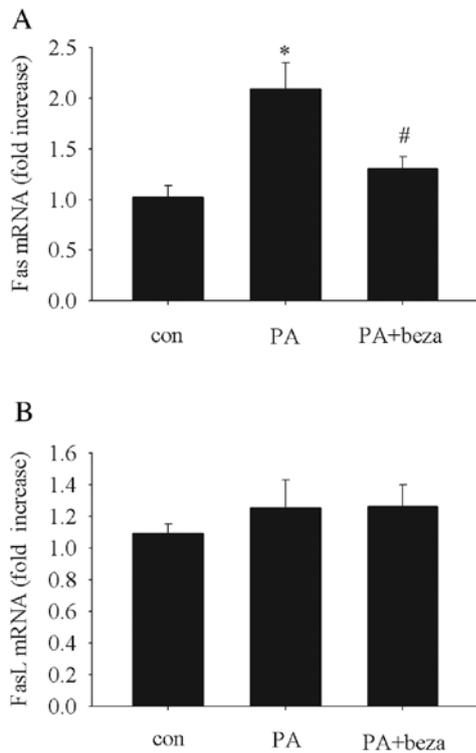
A

B

Figure 4. Effect of palmitate on Fas and FasL mRNA expression in MC3T3-E1 cells. The cells were treated with 500 μM palmitate in the presence or absence of 500 μM bezafibrate for 24 h. (A) The level of Fas and (B) FasL mRNA expression was determined using real-time PCR. Data are normalized to the average value of control and expressed as the mean ± SEM. (n=3). *P<0.05 vs. control; #P<0.05 vs. palmitate alone.

decrease and inhibited palmitate-induced cleaved caspase-3 increase. Taken together, these results suggest that palmitate induces cell apoptosis partly via NF-κB activation in MC3T3-E1 cells.

Effect of bezafibrate on palmitate-induced activation of NF-κB in MC3T3-E1 cells. To investigate whether bezafibrate inhibits palmitate-induced NF-κB activation, we measured the protein levels of IκBα, the nuclear translocation of NF-κB p65 and the protein expression of NF-κB p65 in the nuclear protein extracts from cells treated with palmitate in the presence or absence of bezafibrate. The IκBα protein levels were decreased by 49% with palmitate treatment and bezafibrate restored the palmitate-induced IκBα protein degradation by 89% (Fig. 7C). MC3T3-E1 cells stimulated with palmitate showed a dramatic increase in the translocation of NF-κB p65 into the nucleus (Fig. 7A). In contrast, the palmitate-induced translocation of NF-κB p65 to the nucleus was markedly inhibited by bezafibrate (Fig. 7A). To further confirm the results of immunofluorescence microscopy, we measured the NF-κB p65 expression in nuclear extracts using Western blotting. Palmitate significantly increased nuclear NF-κB p65 expression by 2.08-fold compared to the control group (Fig. 7B). In contrast, pre-treatment with bezafibrate for 2 h markedly inhibited the palmitate-induced nuclear NF-κB p65 expression. These results are consistent with the results of immunofluorescence microscopy. Taken together, these results suggest that bezafibrate inhibited the palmitate-induced NF-κB activation.
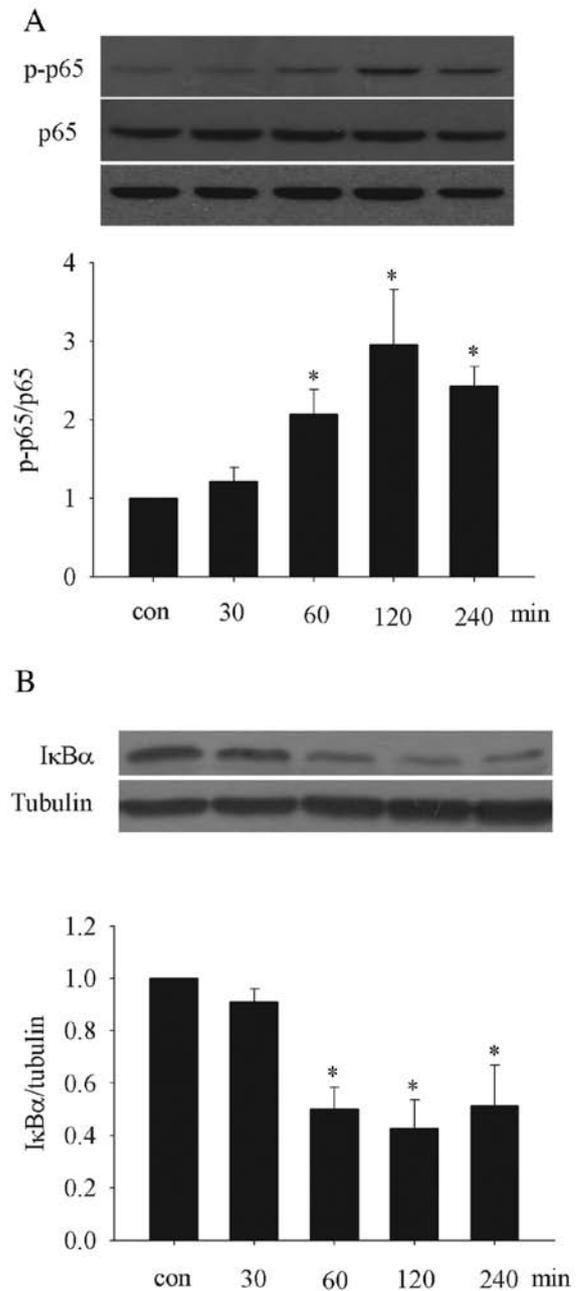
A

B

Figure 5. Effect of palmitate on p-NF-κB p65 and IκBα in MC3T3-E1 cells. The cells were treated with 500 μM palmitate for the indicated duration. Levels of (A) p-NF-κB p65, NF-κB p65 and (B) IκBα protein expression were determined using Western blot analysis. Data are normalized to the average value of the control and are expressed as the mean ± SEM. (n=3). *P<0.05 vs. control.

Discussion

In the present study, we found that palmitate-induced apoptosis in osteoblastic MC3T3-E1 cells was mediated predominantly by NF-κB activation, as well as up-regulation of Fas expression. We also showed that bezafibrate attenuated palmitate-induced apoptosis by inhibiting the NF-κB signaling pathway.

High concentrations of long chain SFAs inhibit cell proliferation and lead to cell death in cultured neonatal rat cardiomyocytes (22) and pancreatic β-cells (23), which are demonstrated by signs of apoptosis, including DNA laddering
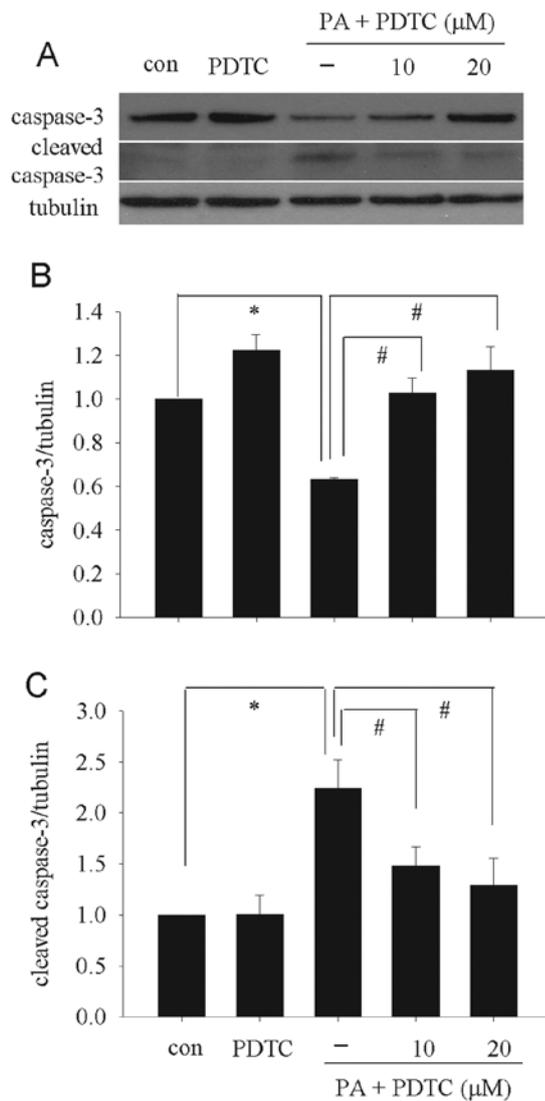
Figure 6. Effect of the NF-κB inhibitor PDTC on palmitate-induced cleaved caspase-3 in MC3T3-E1 cells. The cells were treated with 500 μM palmitate in the presence or absence of 10 or 20 μM PDTC for 24 h. (A) Levels of caspase-3 and cleaved caspase-3 expression were determined using Western blot analysis. (B) Quantification of caspase-3 and (C) cleaved caspase-3 protein expression levels are shown. Data are normalized to the average value of the control and are expressed as the mean ± SEM. (n=3). *P<0.05 vs. control; #P<0.05 vs. palmitate alone.

and caspase activation. It has also been indicated that palmitate induces apoptosis in hFOB1.19, a human fetal osteoblastic cell line (12). In agreement with previous studies, we have shown that palmitate induced apoptosis in osteoblastic MC3T3-E1 cells, suggesting that apoptosis of osteoblasts is an important factor in the reduced BMD induced by a HFD in mice (11).

The mechanism by which palmitate induces apoptosis in osteoblasts has not been fully characterized. Ceramide, reactive oxygen species (ROS), and NF-κB activation have all been implicated in the pathogenesis of fatty acid-induced apoptosis in various settings; however, their relative role may be cell-type dependent. The ceramide synthase inhibitor fumonisin B1 and the anti-oxidant GSH did not inhibit palmitate-induced apoptosis in osteoblasts (12), even though ceramide and ROS are mediators of palmitate-induced apoptosis in pancreatic β-cells. It has also been shown that NF-κB activation is

involved in palmitate-induced apoptosis. For example, in human umbilical vein endothelial cells, saturated NEFAs induce lipoapoptosis via IκB kinase (IKK) and NF-κB. Furthermore, pharmacological inhibition of NF-κB and IKK also blocked stearate-induced apoptosis (24). INS-1 pancreatic β-cells had a prominent sensitivity towards fatty acid-induced apoptosis, resulting in an about 6-fold increase in caspase-3 activation. Reduction of apoptosis by an inhibitor of IKK indicated the involvement of the NF-κB pathway in palmitate-induced apoptosis (25). In the present study, we have also shown that palmitate induced degradation of IκBα and stimulated nuclear translocation of NF-κB p65 in osteoblastic MC3T3-E1 cells. In order to further confirm that palmitate-induced apoptosis is related to NF-κB, we demonstrated that the inhibitor of NF-κB, PDTC, attenuates palmitate-induced caspase-3 activity. NF-κB is an essential transcription factor in the control of expression of genes involved in cell growth, differentiation, and inflammation. Activation of NF-κB has been linked to apoptosis, with the factor playing either an anti-apoptotic or a pro-apoptotic role, depending on the type of cell and the apoptotic stimulus (26). In contrast, another study has shown that SFA promoted osteoclast survival by preventing apoptosis. The stimulation of osteoclast survival in SFA-treated osteoclasts was induced via the Toll-like receptor 4 (TLR4) and NF-κB activation (27). These observations suggest that activation of NF-κB causes palmitate-induced apoptosis in osteoblasts and palmitate-induced survival in osteoclasts.

An important apoptotic signaling pathway involves the Fas-FasL cell death-inducing system. Fas is a 45 kDa membrane protein that triggers apoptosis when interacting with FasL. Fas has already been shown to be expressed in mature osteobasts, in which it induces apoptosis and suppresses differentiation (28). Fas and FasL are up-regulated by various factors including TNFα. Several reports have pointed to Fas and FasL as important regulators of NF-κB-mediated apoptosis, such as, in macrophages and Kupffer cells, NF-κB is reported to regulate Fas-induced apoptosis (29). A previous study has shown that NF-κB is involved in the up-regulation of Fas as early as at the transcriptional level (30), whereas JNK, ERK, and p38 seem to not be essential (31). Osteoblasts isolated from bone samples from postmenopausal women express higher levels of the inflammatory receptor Fas and they are more sensitive to FasL-induced cell death compared to samples from healthy young women (32). In MC3T3-E1 cells, the combination of cytokines (TNF-α, IL-1β and IFN-γ) allowed massive Fas-mediated apoptosis (33). Another animal study (34) has also shown that the level of Fas mRNA seem to be the main regulatory effect of estrogen withdrawal in bone cells, as the expression of FasL in bone cells was not affected by ovariectomy in the osteoblastogenic culture. Our results are consistent with their reports and found that the expression of Fas mRNA in MC3T3-E1 cells was significantly increased with palmitate-treatment, while the expression of FasL was unchanged. In contrast, it has been shown that FasL up-regulation is dependent on NF-κB transcriptional activation by using a FasL promoter reporter assay (29). This could be explained by the fact that FasL is expressed predominantly in activated T lymphocytes (35) and NK cells (36), not in osteoblasts. Therefore, it is possible that the palmitate-induced apoptosis via NF-κB is mediated by Fas in MC3T3-E1 cells.
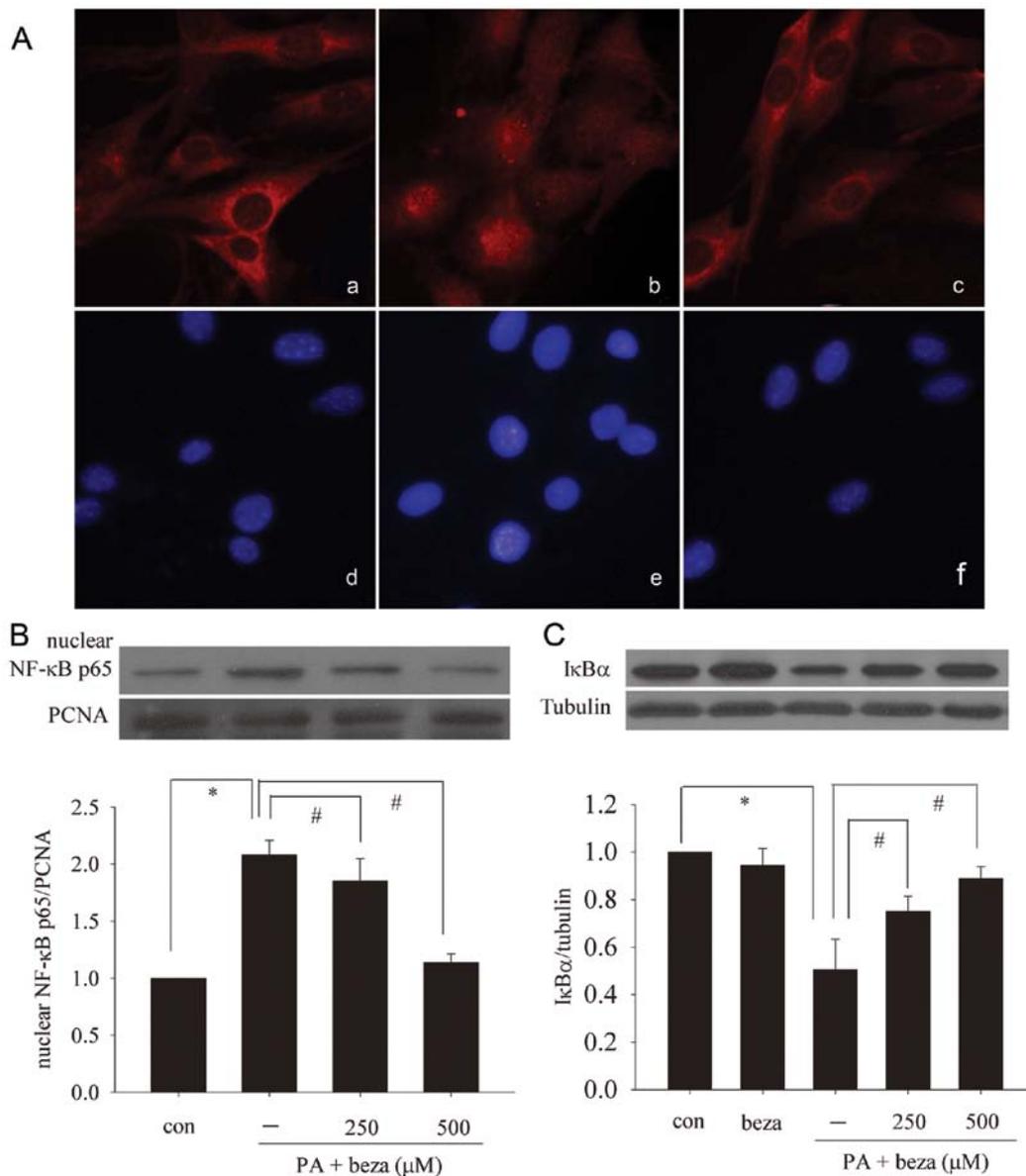
and Yi Yang from the Department of Pharmacology, Sun Yat-sen University for their unselfish technical assistance.

References

1. Salari Sharif P, Abdollahi M and Larijani B: Current, new and future treatments of osteoporosis. Rheumatol Int 31: 289-300, 2011.
2. Kousteni S, Bellido T, Plotkin LI, *et al*: Nongenotropic, sex-nonspecific signaling through the estrogen or androgen receptors: dissociation from transcriptional activity. Cell 104: 719-730, 2001.
3. Weinstein RS, Jilka RL, Parfitt AM and Manolagas SC: Inhibition of osteoblastogenesis and promotion of apoptosis of osteoblasts and osteocytes by glucocorticoids. Potential mechanisms of their deleterious effects on bone. J Clin Invest 102: 274-282, 1998.
4. Eberhardt AW, Yeager-Jones A and Blair HC: Regional trabecular bone matrix degeneration and osteocyte death in femora of glucocorticoid-treated rabbits. Endocrinology 142: 1333-1340, 2001.
5. Legrand P and Rioux V: The complex and important cellular and metabolic functions of saturated fatty acids. Lipids 45: 941-946, 2010.
6. Mittendorfer B, Liem O, Patterson BW, Miles JM and Klein S: What does the measurement of whole-body fatty acid rate of appearance in plasma by using a fatty acid tracer really mean? Diabetes 52: 1641-1648, 2003.
7. Corwin RL, Hartman TJ, Maczuga SA and Graubard BI: Dietary saturated fat intake is inversely associated with bone density in humans: analysis of NHANES III. J Nutr 136: 159-165, 2006.
8. Orchard TS, Cauley JA, Frank GC, *et al*: Fatty acid consumption and risk of fracture in the Women's Health Initiative. Am J Clin Nutr 92: 1452-1460, 2010.
9. Makovey J, Chen JS, Hayward C, Williams FMK and Sambrook PN: Association between serum cholesterol and bone mineral density. Bone 44: 208-213, 2009.
10. Cao JJ, Sun L and Gao H: Diet-induced obesity alters bone remodeling leading to decreased femoral trabecular bone mass in mice. Ann NY Acad Sci 1192: 292-297, 2010.
11. Halade GV, Rahman MM, Williams PJ and Fernandes G: High fat diet-induced animal model of age-associated obesity and osteoporosis. J Nutr Biochem 21: 1162-1169, 2010.
12. Kim JE, Ahn MW, Baek SH, *et al*: AMPK activator, AICAR, inhibits palmitate-induced apoptosis in osteoblast. Bone 43: 394-404, 2008.
13. Cacicedo JM, Benjachareowong S, Chou E, Ruderman NB and Ido Y: Palmitate-induced apoptosis in cultured bovine retinal pericytes: roles of NAD(P)H oxidase, oxidant stress, and ceramide. Diabetes 54: 1838-1845, 2005.
14. Kitajima I, Soejima Y, Takasaki I, Beppu H, Tokioka T and Maruyama I: Ceramide-induced nuclear translocation of NF-kappaB is a potential mediator of the apoptotic response to TNF-alpha in murine clonal osteoblasts. Bone 19: 263-270, 1996.
15. Mogi M, Ozeki N, Nakamura H and Togari A: Dual roles for NF-kappaB activation in osteoblastic cells by serum deprivation: osteoblastic apoptosis and cell-cycle arrest. Bone 35: 507-516, 2004.
16. Meier CR, Schlienger RG, Kraenzlin ME, Schlegel B and Jick H: HMG-CoA reductase inhibitors and the risk of fractures. JAMA 283: 3205-3210, 2000.
17. Wang GJ, Chung KC and Shen WJ: Lipid clearing agents in steroid-induced osteoporosis. J Formos Med Assoc 94: 589-592, 1995.
18. Still K, Grabowski P, Mackie I, Perry M and Bishop N: The peroxisome proliferator activator receptor alpha/delta agonists linoleic acid and bezafibrate up-regulate osteoblast differentiation and induce periosteal bone formation in vivo. Calcif Tissue Int 83: 285-292, 2008.
19. Bu YH, He YL, Zhou HD, *et al*: Insulin receptor substrate 1 regulates the cellular differentiation and the matrix metallo-peptidase expression of preosteoblastic cells. J Endocrinol 206: 271-277, 2010.
20. Bachar E, Ariav Y, Cerasi E, Kaiser N and Leibowitz G: Neuronal nitric oxide synthase protects the pancreatic beta cell from glucolipotoxicity-induced endoplasmic reticulum stress and apoptosis. Diabetologia 53: 2177-2187, 2010.
21. Iwata E, Nakanishi T, Ogawa N, Ohyama K, Murakami T and Takigawa M: Neurotrophin-3 increases the DNA-binding activities of several transcription factors in a mouse osteoblastic cell line. Biochim Biophys Acta 1311: 85-92, 1996.
22. Leroy C, Tricot S, Lacour B and Grynberg A: Protective effect of eicosapentaenoic acid on palmitate-induced apoptosis in neonatal cardiomyocytes. Biochim Biophys Acta 1781: 685-693, 2008.
23. Chu KY, Lin Y, Hendel A, Kulpa JE, Brownsey RW and Johnson JD: ATP-citrate lyase reduction mediates palmitate-induced apoptosis in pancreatic beta cells. J Biol Chem 285: 32606-32615, 2010.
24. Staiger K, Staiger H, Weigert C, Haas C, Haring HU and Kellerer M: Saturated, but not unsaturated, fatty acids induce apoptosis of human coronary artery endothelial cells via nuclear factor-kappaB activation. Diabetes 55: 3121-3126, 2006.
25. Rakatzi I, Mueller H, Ritzeler O, Tennagels N and Eckel J: Adiponectin counteracts cytokine- and fatty acid-induced apoptosis in the pancreatic beta-cell line INS-1. Diabetologia 47: 249-258, 2004.
26. Kaltschmidt B, Kaltschmidt C, Hofmann TG, Hehner SP, Droge W and Schmitz ML: The pro- or anti-apoptotic function of NF-kappaB is determined by the nature of the apoptotic stimulus. Eur J Biochem 267: 3828-3835, 2000.
27. Oh SR, Sul OJ, Kim YY, *et al*: Saturated fatty acids enhance osteoclast survival. J Lipid Res 51: 892-899, 2010.
28. Kovacic N, Lukic IK, Grcevic D, Katavic V, Croucher P and Marusic A: The Fas/Fas ligand system inhibits differentiation of murine osteoblasts but has a limited role in osteoblast and osteoclast apoptosis. J Immunol 178: 3379-3389, 2007.
29. Peng Y, Gallagher SF, Haines K, Baksh K and Murr MM: Nuclear factor-kappaB mediates Kupffer cell apoptosis through transcriptional activation of Fas/FasL. J Surg Res 130: 58-65, 2006.
30. Fujita M, Goto K, Yoshida K, *et al*: Okadaic acid stimulates expression of Fas receptor and Fas ligand by activation of nuclear factor kappa-B in human oral squamous carcinoma cells. Oral Oncol 40: 199-206, 2004.
31. Starace D, Riccioli A, D'Alessio A, *et al*: Characterization of signaling pathways leading to Fas expression induced by TNF-alpha: pivotal role of NF-kappaB. FASEB J 19: 473-475, 2005.
32. Xing L and Boyce BF: Regulation of apoptosis in osteoclasts and osteoblastic cells. Biochem Biophys Res Commun 328: 709-720, 2005.
33. Ozeki N, Mogi M, Nakamura H and Togari A: Differential expression of the Fas-Fas ligand system on cytokine-induced apoptotic cell death in mouse osteoblastic cells. Arch Oral Biol 47: 511-517, 2002.
34. Kovacic N, Grcevic D, Katavic V, *et al*: Fas receptor is required for estrogen deficiency-induced bone loss in mice. Lab Invest 90: 402-413, 2010.
35. Nagata S and Golstein P: The Fas death factor. Science 267: 1449-1456, 1995.
36. Eischen CM, Schilling JD, Lynch DH, Krammer PH and Leibson PJ: Fc receptor-induced expression of Fas ligand on activated NK cells facilitates cell-mediated cytotoxicity and subsequent autocrine NK cell apoptosis. J Immunol 156: 2693-2699, 1996.
37. Peters JM, Aoyama T, Burns AM and Gonzalez FJ: Bezafibrate is a dual ligand for PPARalpha and PPARbeta: studies using null mice. Biochim Biophys Acta 1632: 80-89, 2003.
38. Zanetti M, Stocca A, Dapas B, *et al*: Inhibitory effects of fenofibrate on apoptosis and cell proliferation in human endothelial cells in high glucose. J Mol Med 86: 185-195, 2008.
39. Rival Y, Beneteau N, Taillandier T, *et al*: PPARalpha and PPARdelta activators inhibit cytokine-induced nuclear translocation of NF-kappaB and expression of VCAM-1 in EAhy926 endothelial cells. Eur J Pharmacol 435: 143-151, 2002.
40. Delerive P, De Bosscher K, Besnard S, *et al*: Peroxisome proliferator-activated receptor alpha negatively regulates the vascular inflammatory gene response by negative cross-talk with transcription factors NF-kappaB and AP-1. J Biol Chem 274: 32048-32054, 1999.
41. Jove M, Laguna JC and Vazquez-Carrera M: Agonist-induced activation releases peroxisome proliferator-activated receptor beta/delta from its inhibition by palmitate-induced nuclear factor-kappaB in skeletal muscle cells. Biochim Biophys Acta 1734: 52-61, 2005.
42. Okamoto H, Iwamoto T, Kotake S, Momohara S, Yamanaka H and Kamatani N: Inhibition of NF-kappaB signaling by fenofibrate, a peroxisome proliferator-activated receptor-alpha ligand, presents a therapeutic strategy for rheumatoid arthritis. Clin Exp Rheumatol 23: 323-330, 2005.